

Theory for the electronic structure of high- T_c superconductors

G. Baumgärtel, J. Schmalian, and K.-H. Bennemann

Institute for Theoretical Physics, Freie Universität Berlin, Arnimallee 14, 1000 Berlin 33, Germany

(Received 18 February 1993)

Using a three-band Hubbard Hamiltonian within a slave-boson mean-field approximation we determine the doping dependence of the density of states in the CuO_2 planes. We analyze in detail the occurrence of local magnetic moments, their effects on the electronic structure, and the insulating state resulting from a charge transfer or a Mott-Hubbard gap. This theory permits a treatment of highly correlated systems over the whole doping range and thus of the transition from local moment to fully itinerant behavior. Using the density of states various magnetic, spectroscopic, and transport properties are calculated. Our analysis sheds light on the difference of electron versus hole doping and in particular on the doping dependence of the Cu-O singlet and the Hall coefficient. More generally, by comparing with experimental data and theoretical results obtained by alternative methods one learns more about the validity of the slave-boson mean-field theory. We also discuss how the theory can be extended to include quantum fluctuations.

I. INTRODUCTION

The spectral density of the carrier states in high- T_c superconductors is of central interest with regards to an understanding of the electronic properties of these materials. Experimental results suggest a complicated interplay between itinerant holes (electrons) and localized Cu spins. The long-range antiferromagnetism depends sensitively on the carrier concentration and exhibits an asymmetric dependence on electron or hole doping.¹ NMR and neutron-scattering experiments indicate the existence of magnetic correlations in the paramagnetic phase of the cuprates.^{2,3} Measurements of the optical conductivity in La_2CuO_4 and Pr_2CuO_4 yield charge transfer gaps of the order of 1.8 eV and 1.4 eV, respectively.⁴ These are also observed by O 1s x-ray-absorption spectroscopy (XAS) (Ref. 5) and electron-energy-loss spectroscopy (EELS).⁶ The insulator-metal transition and the doping dependence of the p and d character of the states at the Fermi energy E_F and of E_F itself are presently studied intensively.^{7,8} In particular, the latter problem is under debate due to conflicting experimental observations.

It is therefore important to develop an electronic theory for the cuprates which is valid over a large doping range and can describe localized behavior of the charge carriers for small doping and strongly itinerant behavior for larger doping. Furthermore, it is of interest to determine the character of the elementary excitations and to clarify whether it is possible to explain experimental data within a quasiparticle picture.

In order to obtain a better understanding of the spectral density several groups have studied the two-dimensional Hubbard Hamiltonian and the t - J model by diagonalizing small clusters exactly⁹⁻¹³ or by using the quantum Monte Carlo method.¹⁴⁻¹⁶ These calculations show clearly the importance of strong correlations

for the electronic structure, in particular for the metal-insulator transition and for the doping dependence of the distribution of spectral weight. Interestingly, these studies also show that the energy dispersion of the quasiparticles near the Fermi level resembles the dispersion obtained in local-density-approximation¹⁷ (LDA) calculations. Still, there are many open questions concerning, for example, the relative weights of p and d states in the various bands, the corresponding asymmetric behavior of the antiferromagnetic phase upon hole or electron doping, and the effects of finite temperatures. In addition, it is very intriguing that Hall measurements¹⁸⁻²⁰ of moderately doped high- T_c systems yield small carrier concentrations, while angular resolved photoemission studies²¹⁻²³ (ARPES's) and angular resolved inverse photoemission experiments²⁴ (ARIPES's) find a large Fermi surface.

The main goal of our paper is to present a theory for the normal state of the CuO_2 planes which covers the whole doping range and is able to treat local magnetic moments^{25,26} and the transition to itinerant behavior. Within a slave-boson mean-field approximation to the three-band Hubbard Hamiltonian we study the effects of magnetic moments on the density of states, the dispersion of the bands, and the metal-insulator transition. We also investigate spin-singlet formation and the doping dependence of the distribution of spectral weight, of the Fermi energy and Fermi surface, and of the Hall coefficient. If we take into account charge and spin fluctuations of the slave bosons beyond their mean-field values, then this theory extends and includes our previous one for elementary excitations in itinerant systems²⁷ and one expects to get a workable theory for a variety of normal-state properties of high- T_c superconductors.

Here, we present results of the mean-field version of our theory. Since we determine self-consistently the occurrence of local magnetic moments on the copper sites,^{28,29}

we can study systematically their effects on the density of states and related properties. We obtain that local magnetic moments drive the metal-insulator transition due to a charge-transfer gap and cause the formation of a ligand hole band (“spin-singlet band”) which has a LDA-type dispersion. Upon hole doping the Fermi level moves into the singlet band. For increasing hole or electron doping the amplitude of the local moments decreases and vanishes for $x \approx 0.4$, reflecting a transition to the itinerant regime. These results for the change of the density of states with doping are compared in detail with XAS, EELS, and photoemission experiments. It is very interesting that our effective mean-field theory agrees with many experimental data and with important results found in exact cluster calculations. Thus, we believe that this model is a good starting point for further investigation of relevant problems such as the magnetic phase diagram and elementary excitations. For example, our three-band theory is able to explain the difference between electron and hole doping³⁰ observed in the anti-ferromagnetic phase and the unusual doping and temperature dependence of the static spin susceptibility.³¹ From comparison with experiment and alternative calculations we also see the shortcomings of our theory with respect to many-particle excitations. However, we can address a variety of problems which are not easily accessible to exact cluster calculations.

In Sec. II we first describe the slave-boson transformation and the approximations made to obtain a workable mean-field theory. Then we sketch briefly how the theory can be improved by the inclusion of quantum fluctuations of the bosons. In Sec. III we present our results and critically discuss the validity of our model. In Sec. IV we indicate the implications of our results and discuss the potential of our model concerning the understanding of the magnetic phase diagram and the static spin susceptibility.

II. THEORY

We start from the three-band Hubbard Hamiltonian for the Cu $3d_{x^2-y^2}$ and O $2p_{x,y}$ orbitals in the CuO₂ planes:

$$H = \sum_{j,\sigma} (\varepsilon_d^0 - \mu) f_{j\sigma}^\dagger f_{j\sigma} + \sum_{i,\sigma,\alpha} (\varepsilon_p - \mu) p_{i\sigma\alpha}^\dagger p_{i\sigma\alpha} + t \sum_{ij,\sigma,\alpha} \gamma_{ij} (p_{i\sigma\alpha}^\dagger f_{j\sigma} + \text{H.c.}) + U \sum_j f_{j\uparrow}^\dagger f_{j\uparrow} f_{j\downarrow}^\dagger f_{j\downarrow}. \quad (1)$$

Here, $f_{l\sigma}^\dagger$ ($p_{l\sigma\alpha}^\dagger$) creates a hole at a Cu (O) site l with spin σ and ε_d^0 (ε_p) are the corresponding on-site energies. t is the nearest-neighbor Cu-O hopping integral, U is the Coulomb repulsion between Cu holes, and μ is the chemical potential of the system. The $p_x - d$ and $p_y - d$ hopping matrix elements $t\gamma_{ij}$ alternate in sign in the x and y directions, respectively.³² In the following we use the parameters $\Delta = \varepsilon_p - \varepsilon_d^0 = 3\text{eV}$, $U = 8\text{eV}$, and $t = 1.1\text{eV}$ for hole-doped superconductors and $\Delta = 2.4\text{eV}$, $U = 8\text{eV}$, and $t = 0.96\text{eV}$ for

electron-doped superconductors, where Δ/t and U/t are taken from recent cluster³³ and quantum Monte Carlo¹⁶ calculations.

In order to treat the effects of strong electronic correlations, we use the spin-rotation-invariant formulation³⁴ of the slave-boson method of Kotliar and Ruckenstein.³⁵ In this approach, one introduces pseudofermions $d_{j\sigma}$ and auxiliary bosons e_j , $s_{j\sigma\sigma'}$, and δ_j , which label the empty, singly occupied, and doubly occupied states on a Cu site in an enlarged Hilbert space, respectively. The atomic states at site j corresponding to the empty site, the singly occupied site with spin σ , and the doubly occupied site are then obtained from

$$|0j\rangle = e_j^\dagger |\text{vac}\rangle, \quad (2a)$$

$$|\sigma j\rangle = \sum_{\sigma'} s_{j\sigma\sigma'}^\dagger d_{j\sigma'}^\dagger |\text{vac}\rangle, \quad (2b)$$

$$|\uparrow\downarrow j\rangle = \delta_j^\dagger d_{j\uparrow}^\dagger d_{j\downarrow}^\dagger |\text{vac}\rangle, \quad (2c)$$

where the pseudofermions $d_{j\sigma}$ are related to the original fermions $f_{j\sigma}$ via

$$f_{j\sigma}^\dagger = \sum_{\sigma'} z_{j,\sigma\sigma'}^\dagger d_{j\sigma'}^\dagger. \quad (3)$$

The choice of $z_{j,\sigma\sigma'}$ is not unique. Here, we use

$$\underline{z}_j = [(1 - \delta_j^\dagger \delta_j) \tau_0 - \underline{s}_j^\dagger \underline{s}_j]^{-1/2} (e_j^\dagger \underline{s}_j + \tilde{\underline{s}}_j^\dagger \delta_j) \times [(1 - e_j^\dagger e_j) \tau_0 - \tilde{\underline{s}}_j^\dagger \tilde{\underline{s}}_j]^{-1/2}, \quad (4)$$

which leads to the well-known Gutzwiller approximation in the Pauli-paramagnetic saddle-point approximation.^{34,35} The matrix structure of the boson $s_{j\sigma\sigma'}^\dagger = (\underline{s}_j^\dagger)_{\sigma\sigma'}$ is necessary to preserve the spin-rotation invariance of the original Hamiltonian. Usually \underline{s}_j^\dagger is represented by its projections onto the Pauli matrices $\boldsymbol{\tau} = (\tau_x, \tau_y, \tau_z)$ and the unit matrix τ_0 so that $s_{j\mu}^\dagger = \frac{1}{\sqrt{2}} \text{tr}(\tau_\mu \underline{s}_j)$. The operator $\tilde{\underline{s}}_j$ is the time reversed complement of \underline{s}_j . Since e_j , s_{j0} , $\mathbf{s}_j = (s_{jx}, s_{jy}, s_{jz})$, and δ_j obey bosonic commutation relations, there are unphysical states in the new Hilbert space which are eliminated by the local constraints

$$Q_j \equiv e_j^\dagger e_j + s_{j0}^\dagger s_{j0} + \mathbf{s}_j^\dagger \cdot \mathbf{s}_j + \delta_j^\dagger \delta_j - 1 = 0, \quad (5a)$$

$$n_j^d \equiv s_{j0}^\dagger s_{j0} + \mathbf{s}_j^\dagger \cdot \mathbf{s}_j + 2\delta_j^\dagger \delta_j = \sum_\sigma d_{j\sigma}^\dagger d_{j\sigma}, \quad (5b)$$

$$\mathbf{m}_j \equiv s_{j0}^\dagger \mathbf{s}_j + \mathbf{s}_j^\dagger s_{j0} + i(\mathbf{s}_j^\dagger \times \mathbf{s}_j) = \sum_{\sigma\sigma'} d_{j\sigma}^\dagger \boldsymbol{\tau}_{\sigma\sigma'} d_{j\sigma'}. \quad (5c)$$

The Hamiltonian of Eq. (1) can now be written in terms of the pseudofermion and slave-boson operators as

$$H = H_{\text{eff}} + \sum_j \{U \delta_j^\dagger \delta_j + \nu_j Q_j - \lambda_{0j} n_j^d + \boldsymbol{\lambda}_j \cdot \mathbf{m}_j\}. \quad (6)$$

The effective Hamiltonian H_{eff} which does not contain direct fermion-fermion interactions is given by

$$H_{\text{eff}} = \sum_{j,\sigma\sigma'} d_{j\sigma}^\dagger \{ (\varepsilon_d^0 - \mu + \lambda_{0j}) \tau_{0\sigma\sigma'} - \lambda_j \cdot \tau_{\sigma\sigma'} \} d_{j\sigma'} + \sum_{i,\sigma,\alpha} (\varepsilon_p - \mu) p_{i\sigma\alpha}^\dagger p_{i\sigma\alpha} + t \sum_{ij,\sigma\sigma',\alpha} \gamma_{ij} (p_{i\sigma\alpha}^\dagger z_{j,\sigma\sigma'} d_{j\sigma'} + \text{H.c.}). \quad (7)$$

ν_j , λ_{0j} , and λ_j are Lagrange multipliers which act as internal molecular fields and $z_{j,\sigma\sigma'}$ takes the bosonic hopping processes into account that accompany any fermionic hopping.

The advantage of the slave-boson formulation is the possibility to perform nonperturbative approximations which are not limited to specific values of U/t . One powerful approach is the expansion of the thermodynamical potential with respect to the number of closed boson loops. In zeroth order this is equivalent to the static saddle-point approximation. In this mean-field approximation one neglects the quantum fluctuations of the bosons which are assumed to be numbers.

In the following, we study in detail the mean-field approach which is a prerequisite for any systematic inclusion of quantum fluctuations. Consequently, H_{eff} is an

effective single-particle Hamiltonian with renormalized on-site energy and hopping element. The molecular fields λ_{0j} and λ_j are determined self-consistently by a minimization of the ground-state energy of the Hamiltonian in Eq. (6). Concerning the treatment of H_{eff} at the saddle point this extends our previous theory²⁷ which assumed $\lambda_j = 0$ appropriate for itinerant systems with larger doping. As usual λ_{0j} is considered to be site independent. For λ_j we assume at each site $\lambda_j = \pm(0, 0, \Lambda)$ with equal probability so that $z_{j\sigma\sigma'} = z_{j\sigma} \delta_{\sigma\sigma'}$. The fictitious alloy resulting from the random distribution of magnetic molecular fields is treated within the single-site coherent-potential approximation (CPA) (Refs. 25 and 28) by applying the CPA formulation due to Shiba^{36,37} to the three-band Hubbard model. We then obtain from H_{eff} the d -state contribution to the spin-resolved density of states at a site j with a given molecular field λ_j which is embedded in the CPA medium:

$$\varrho_{dj\sigma}(\omega) = -\frac{1}{\pi} \text{Im} \left\{ \frac{1}{z_{j\sigma}} [F(\omega)^{-1} + E_{j\sigma}(\omega) - \mathcal{L}(\omega)]^{-1} \right\}. \quad (8)$$

For the density of states, $\varrho_{pj\sigma}(\omega) = \frac{1}{2} \sum_{i \text{ NN } j} \varrho_{pi\alpha}$, of the oxygen sites around a Cu site j with a given molecular field λ_j , we obtain

$$\varrho_{pj\sigma}(\omega) = -\frac{1}{\pi} \text{Im} \left\{ \frac{1}{\omega - \varepsilon_p} \left(2 + \frac{2t^2}{\omega - \varepsilon_p} F(\omega) + \frac{(\mathcal{L}(\omega) - \frac{2t^2}{\omega - \varepsilon_p}) F(\omega) \frac{2t^2}{\omega - \varepsilon_p} [\mathcal{L}(\omega) - E_{j\sigma}(\omega)] F_{j(i)}^2(\omega) - 1}{1 + [E_{j\sigma}(\omega) - \mathcal{L}(\omega)] F(\omega)} \right) \right\}. \quad (9)$$

Here, the coherent locator $\mathcal{L}(\omega)$ is the generalization of the CPA self-energy for a system with off-diagonal disorder (resulting from the $z_{j\sigma}$). It describes the effective medium of the holes and is determined from the CPA condition

$$F(\omega) = \left\langle [F(\omega)^{-1} + E_{j\sigma}(\omega) - \mathcal{L}(\omega)]^{-1} \right\rangle_c. \quad (10)$$

$\langle \dots \rangle_c$ refers to averaging with respect to λ_j , $E_{j\sigma}(\omega) = (\omega - \varepsilon_d^0 - \lambda_0 + \sigma \lambda_{jz}) / z_{j\sigma}^2$, and the auxiliary Green's function $F(\omega)$ is given by

$$F(\omega) = \frac{\omega - \varepsilon_p}{4t^2} \sum_k \frac{1}{(\omega - \varepsilon_p) \mathcal{L}(\omega) / (4t^2) - \gamma_k^2}. \quad (11)$$

The coherence factor $\gamma_k = \sqrt{\sin^2(k_x/2) + \sin^2(k_y/2)}$ describes nearest-neighbor Cu-O hopping processes, where k_x^{-1} and k_y^{-1} are given in units of the Cu-Cu bond length. The intersite Green's function, which is averaged over the nearest copper neighbors of j , reads

$$F_{j(i)}(\omega) = \frac{\omega - \varepsilon_p}{4t^2} - \left(\frac{\mathcal{L}(\omega)(\omega - \varepsilon_p)}{4t^2} - 1 \right) F(\omega)$$

The total copper and oxygen densities of states ϱ_d and ϱ_p are obtained from Eqs. (8) and (9) by averaging with

respect to λ_j . The densities of states are strongly affected by the presence of local moments whose existence and magnitude are determined *self-consistently* by a minimization of the ground-state energy. The existence of local moments in our mean-field theory corresponds to a localized behavior of copper spins on the time scale of the hopping processes.

Note that $\varrho_d(\omega)$ is the (normalized) density of states of the pseudofermions $d_{j\sigma}$. As in any slave-boson mean-field approach the density of states of the original fermions, $-\frac{1}{\pi} \text{Im} F(\omega)$, is not normalized because the constraints of Eqs. (5) are fulfilled only on average. However, the transformation $d_{j\sigma} \rightarrow f_{j\sigma}$ will not change the position of the bands since $\text{Im}(z_{j\sigma}) = 0$ in our mean-field theory. Furthermore, we obtain only a slight renormalization³⁸ of the hopping ($z_{j\sigma} \approx 1$), and there is solely a small difference between original fermions and pseudofermions so that $\varrho_d(\omega) \approx -\frac{1}{\pi} \text{Im} F(\omega)$. Obviously, the p states are not affected by the slave-boson transformation and the $p_{i\sigma\alpha}$ describe still original fermions. The Fermi energy is determined from the total number of particles, $n = -d\langle H \rangle / d\mu$. Thus, it follows from Eqs. (6) and (7) that E_F is the Fermi energy of the $p_{i\sigma\alpha}$ and $d_{j\sigma}$. In the following, we consider for the Cu states only the pseudofermions, bearing in mind that this does not affect the principal structure of the density of states. It is of course

tempting to speculate that the missing states of the original fermions belong to the incoherent part of the spectrum which cannot be described in a quasiparticle picture.

We derived that the local densities of states, $\varrho_{d(p)}(\omega)$, of the paramagnetic and antiferromagnetic phases can be expressed by $g_{d(p)}(\omega)\mathcal{K}(h(\omega))$ where the characteristics of the $d(p)$ states are properly weighted by $g_{d(p)}(\omega)$ and

$$\mathcal{K}(z) = \sum_k \frac{1}{z - \gamma_k^2}$$

depends on the function $h(\omega)$ which describes mainly the lattice structure. While $\mathcal{K}(z)$ is approximated³⁹ by $2(z - 1 - \sqrt{z^2 - 2z})$, we use exact expressions for $g_{d(p)}(\omega)$ and $h(\omega)$.

The consideration of Gaussian fluctuations of the bosons around their saddle-point values in the spirit of our previous work [e.g., $e_i(\tau) = e_{i,\text{sp}} + \delta e_i(\tau)$] is straightforward but causes computational problems. The interaction of the fermions with the fluctuating bosons leads to a renormalization of the boson propagator. However, in contrast to the Pauli-paramagnetic case the spin and charge quantum fluctuations are not decoupled. Furthermore, as in the linear-response formulation of the CPA (Ref. 40) one has to include vertex corrections in the boson self-energy. From this one finally obtains a renormalized fermion Green's function. Our results of this approach for the static spin susceptibility indicate an interesting doping and temperature dependence.³¹

For the following numerical analysis, we apply the saddle-point approximation to the effective Hamiltonian of Eq. (7) and calculate the density of states from Eqs. (8) and (9).

III. RESULTS AND DISCUSSION

Using the above theory we present now results for the metal-insulator transition and for the doping dependence of the density of states, of the Cu-O singlet, and of the Fermi surface. We then determine the Hall coefficient and discuss its relation to the energy dispersion of the bands. This should demonstrate whether our approximation yields already important experimental facts and results obtained by other theories.

In Figs. 1 and 2(a) we show results for the dependence of the density of states, $\varrho_{d(p)}(\omega)$, on Δ and U . In the case of a weakly correlated system we obtain a metal. However, if U and Δ are larger than certain critical values U_c and Δ_c , we obtain a Mott-Hubbard insulator for $U < \Delta$ and a charge-transfer insulator for $U > \Delta$.⁴¹ The resultant metal-insulator phase diagram is also shown. Most importantly we obtain in agreement with experimental results a density of states with a charge-transfer gap using parameters Δ and U appropriate for the high- T_c materials. By contrast, for a Pauli-paramagnetic (Brinkmann-Rice) localization,⁴² i.e., $t_{\text{eff}} = z_{i\sigma}t \rightarrow 0$, the critical $\Delta/t \geq 4\sqrt{2 + \frac{8}{\pi^2}} \approx 6.7$ is too large to describe the metal-insulator transition of the cuprates. Our results are supported by a recent variational Monte Carlo calculation⁴³ for the two-dimensional three-band Hubbard model which suggests the absence of a Brinkmann-Rice transition.

Our results also shed light on the *origin* of the spectral density structure, which is strongly influenced by the formation of local magnetic moments. We find that the density of states has two copper-dominated Hubbard bands separated by about U , a nonbonding oxygen band at $\varepsilon_p \equiv 0$, and two oxygen-dominated ligand hole bands in the vicinity of ε_p ; see Fig. 2(a). The ligand hole band below ε_p has mainly bonding character due to the hybridization of oxygen hole states with copper states at $\varepsilon_d^0 + U$ and forms the singlet state. Similarly, the ligand hole band above ε_p has mainly antibonding character due to the hybridization of oxygen hole states with copper states at ε_d^0 and forms the triplet state. Analyzing in more detail the densities of states of the charge transfer [Fig. 2(a)] and the Mott-Hubbard [Fig. 1(b)] insulator we find that for increasing Δ/U the lower ligand hole band of the charge-transfer system changes gradually into an upper Hubbard band. This behavior was also obtained in a recent exact cluster calculation⁴⁴ and shows that our mean-field theory can reproduce the essential features of the bands in the insulating state. Summarizing, our theory yields properly the existence of two Hubbard bands and of two ligand hole bands due to the hybridization of p and d states. The positions of these bands are in surprisingly good agreement with exact calculations^{9,16,33} and experiment.

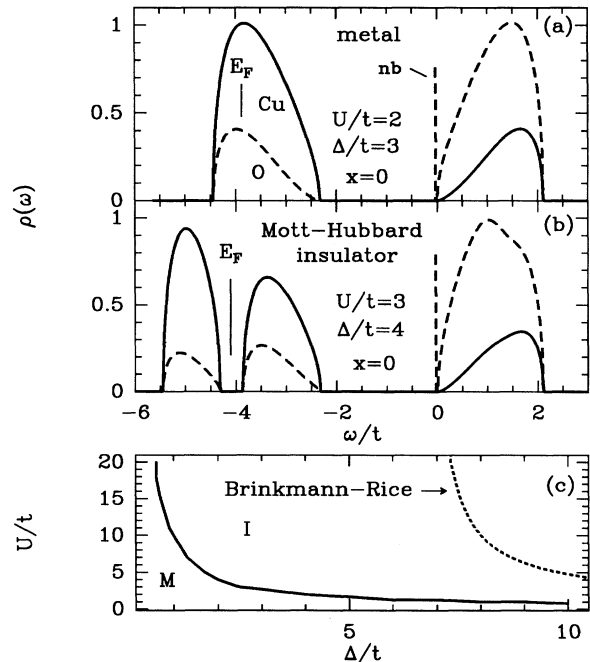


FIG. 1. Results for the copper (solid line) and the oxygen (dashed line) density of states for various Δ and U . The nonbonding oxygen band (nb) at $\varepsilon_p = 0$ is a δ function due to setting the oxygen-oxygen overlap $t_{pp} = 0$. (a) refers to weak correlations yielding a metallic phase and (b) refers to a Mott-Hubbard insulator. In (c) we show the metal-insulator phase diagram resulting from the occurrence of a gap in the density of states (solid line). For comparison the metal-insulator transition due to a Brinkmann-Rice localization ($z_{j\sigma} \rightarrow 0$) is also shown (dashed line).

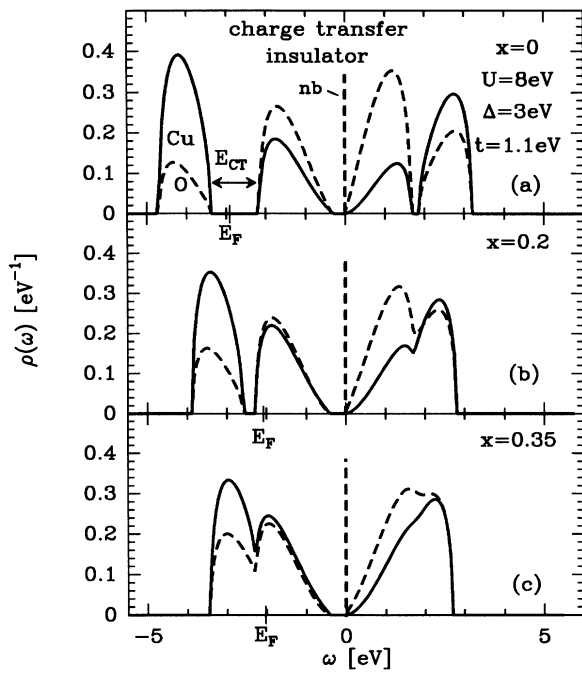


FIG. 2. Dependence of the paramagnetic copper density of states (solid line) and oxygen density of states (dashed line) on hole doping for typical parameter values of high- T_c superconductors. The charge-transfer gap (E_{CT}) is reduced upon doping with holes and disappears at $x = 0.325$.

In Fig. 3 we present results for the spin distribution in the various bands. These refer to a Cu site which “feels” a molecular field $\lambda_j = (0, 0, \Lambda)$. We find the physically very interesting result that the oxygen spin polarization in the lower ligand hole band is predominantly antiparallel to the neighboring Cu spins in the lower Hubbard band, reflecting spin-singlet formation.³² Upon doping

the tendency towards singlet formation gets weaker, but persists up to the disappearance of local moments. The nonbonding oxygen state separates the singlet band from the triplet one above ε_p .

The doping dependence of the density of states shown in Fig. 2 compares satisfactorily with experiment. For $x = 0$ we obtain charge-transfer gaps of 1 eV and 1.2 eV in the local moment phase and of 2 eV and 2.3 eV in the antiferromagnetic phase for electron- and hole-doped systems, respectively (experimental observations at room temperature,⁴ 1.4 eV and 1.8 eV). Upon hole doping the Fermi energy moves first to the bottom of the ligand hole band, whereas for electron-doped systems E_F is close to the top of the lower Hubbard band. This is also observed in XAS (Ref. 5) and EELS (Ref. 6) experiments for $\text{La}_{2-x}\text{Sr}_x\text{CuO}_4$, where the change of the threshold energy due to small hole doping coincides with the observed optical gap of the undoped compound. Upon further doping up to $x = 0.3$ the Fermi energy changes slightly by 0.35 eV (EELS experiment,⁶ 0.3 eV; photoemission experiment for $\text{Bi}_2\text{Sr}_2\text{Ca}_{1-x}\text{Y}_x\text{Cu}_2\text{O}_{8+\delta}$,⁴⁵ 0.4 eV). This weak doping dependence of E_F results from the shrinking of the charge-transfer gap and differs from rigid-band behavior, yielding 0.6 eV. Also, for increasing hole concentration the magnetic moments ($m = 0.68$ for $x = 0$) decrease first slowly up to $x = 0.275$, then rapidly, and disappear for $x \simeq 0.4$. For $x = 0.325$ the gap vanishes and we obtain a single band below ε_p in agreement with EELS experiments.⁶ This justifies our previous assumption of Pauli paramagnetism for larger hole doping. A similar situation occurs for electron doping; see Fig. 4. However, there are important differences concerning the relative change of the Cu and O occupation numbers upon doping. For $|x| = 0.15$ we obtain $\Delta n_d/n_d = 1.8\%$ for hole doping (i.e., the holes go mainly to the oxygen sites) and $\Delta n_d/n_d = 16.7\%$ for electron doping. The latter result agrees well with the reduction of the Cu $2p_{3/2}$ absorption line ($14 \pm 4\%$) determined for $\text{Nd}_{1.85}\text{Ce}_{0.15}\text{CuO}_4$

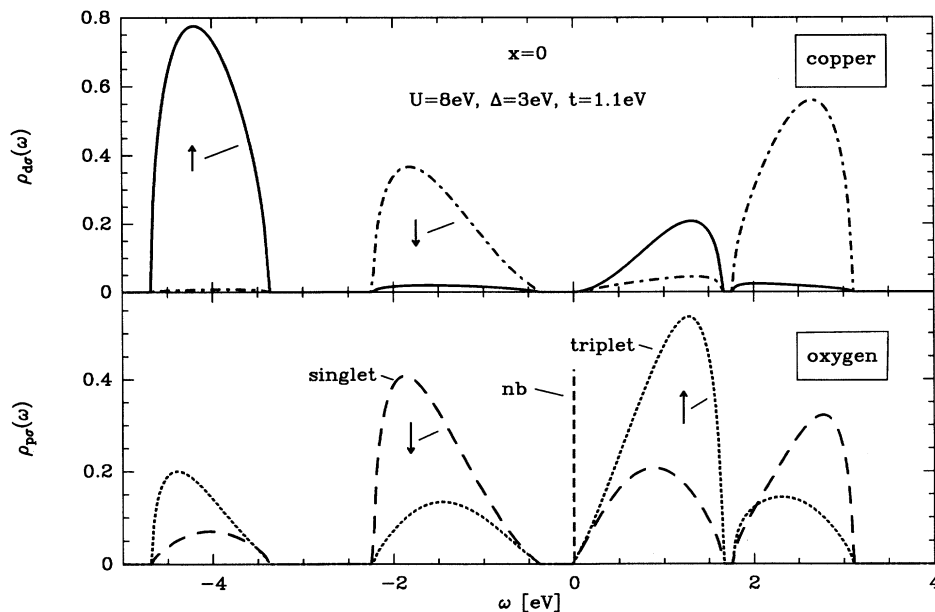


FIG. 3. Results for the spin-dependent copper density of states and for its nearest-neighbor oxygen states at a site with a given molecular field $\lambda = (0, 0, \Lambda)$. The oxygen spins in the ligand hole band below $\varepsilon_p = 0$ are mainly antiparallel to the copper spins in the lower Hubbard band, reflecting singlet formation upon doping.

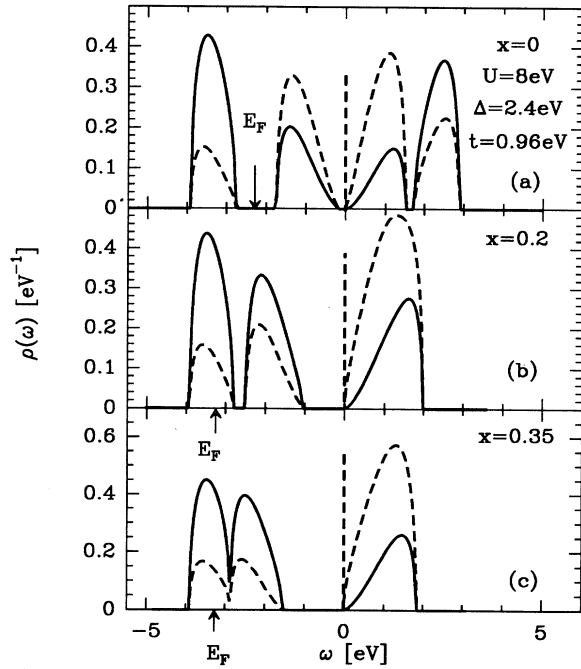


FIG. 4. Dependence of the paramagnetic copper density of states (solid line) and oxygen density of states (dashed line) on electron doping for typical parameter values of high- T_c superconductors.

by EELS.⁴⁶ Comparing with photoemission experiments by Allen *et al.*⁷ it is interesting that we find in agreement with other calculations^{9,16} and recent photoemission studies⁸ no pinning of E_F in the charge-transfer gap.

As can be seen from Figs. 2 and 4 the lower Hubbard band is shifted towards higher energies with increasing hole doping, whereas the singlet band moves towards lower energies for increasing electron doping. This corresponds to a transfer of states in the direction of the band containing the Fermi energy and is related to the transfer of spectral weight found in exact cluster-diagonalization studies¹¹ where the weight of the band at the Fermi level increases with doping. Our mean-field theory yields only a spectral weight transfer resulting from the gradual closing of the gaps between the lower Hubbard band and the singlet band and between the triplet band and the upper Hubbard band, but it does not describe spectral weight transfer across the gaps. Thus, our estimate of the doping dependence of the Fermi energy might need correction. For larger doping when the lower Hubbard band and the singlet band overlap this defect of our theory becomes less important.

In Fig. 5 results are shown for the doping dependence of the Fermi surface determined from the momentum distribution $n(k) = \langle d_{k\sigma}^\dagger d_{k\sigma} + \sum_{\alpha} p_{k\sigma\alpha}^\dagger p_{k\sigma\alpha} \rangle$ and defined by the condition $n(k) = \frac{1}{2}$. We obtain in agreement with exact cluster calculations^{10,44,47} and a recent alloy-analogy approximation of the Hubbard model,⁴⁸ a large Fermi surface fulfilling the Luttinger theorem. In order

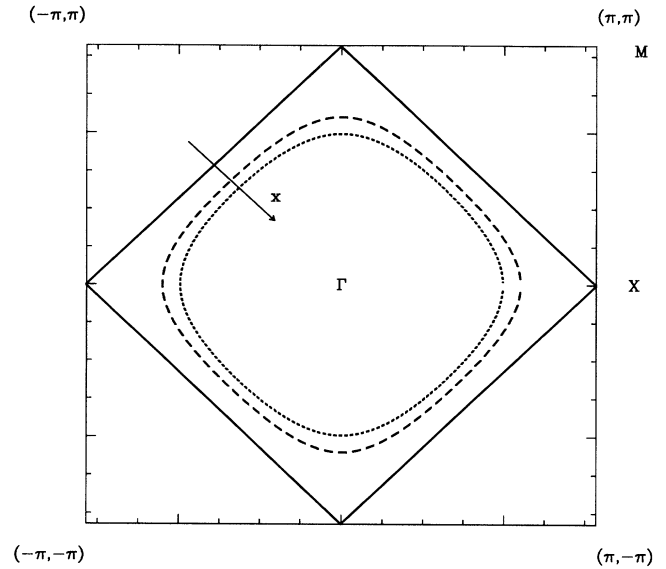


FIG. 5. Doping dependence of the Fermi surface which separates points in momentum space with $n(k) > \frac{1}{2}$ and $n(k) < \frac{1}{2}$. The solid line refers to the hole concentration $x = 0$, the dashed line to $x = 0.2$, and the dotted line to $x = 0.35$.

to understand the existence of a large Fermi surface in a slightly doped charge transfer insulator, note that for a given momentum k the sum of occupied and unoccupied weights is normalized to 1 only if one adds up the contributions from the lower Hubbard band and the lower ligand hole band (or upper Hubbard band and upper ligand hole band), but it is not normalized in one of the subbands. For each k there are then contributions to $n(k)$ from both these bands. Therefore, for small hole doping the existence of states in the lower Hubbard band with $n(k) > \frac{1}{2}$ causes the formation of a large Fermi surface around Γ . In order to illustrate this we show in Fig. 6 the dependence of the momentum distribution $n(k)$ on hole doping. Clearly, the Fermi surface is shifted towards the Γ point for increasing doping. From Fig. 6 it can also be seen that for smaller hole doping ($x < 0.35$) the most significant changes of $n(k)$ occur first near the M point $k = (\pi, \pi)$ ($x < 0.1$) and then near the X point $k = (\pi, 0)$ ($0.1 < x < 0.35$). For larger doping the Fermi surface finally separates regions with $n(k) \simeq 1$ and $n(k) \simeq 0$. These results are in agreement with a recent exact cluster calculation by Ohta *et al.*⁴⁴ and a high-temperature expansion by Singh and Glenister.⁴⁹ In our theory we then obtain for moderate hole doping that the states near the Fermi energy which are progressively filled upon doping are mostly in the vicinity of (π, π) and $(\pi, 0)$ (Ref. 50) and not at the Fermi surface. These states in the lower ligand hole band should mainly determine the density of states at the Fermi energy and the transport properties in hole-doped systems. One may argue similarly in the case of electron doping.

In Fig. 7 we show results for the paramagnetic energy dispersion ε_k in the lower Hubbard band and the lower ligand hole band. Although the momentum k is not a

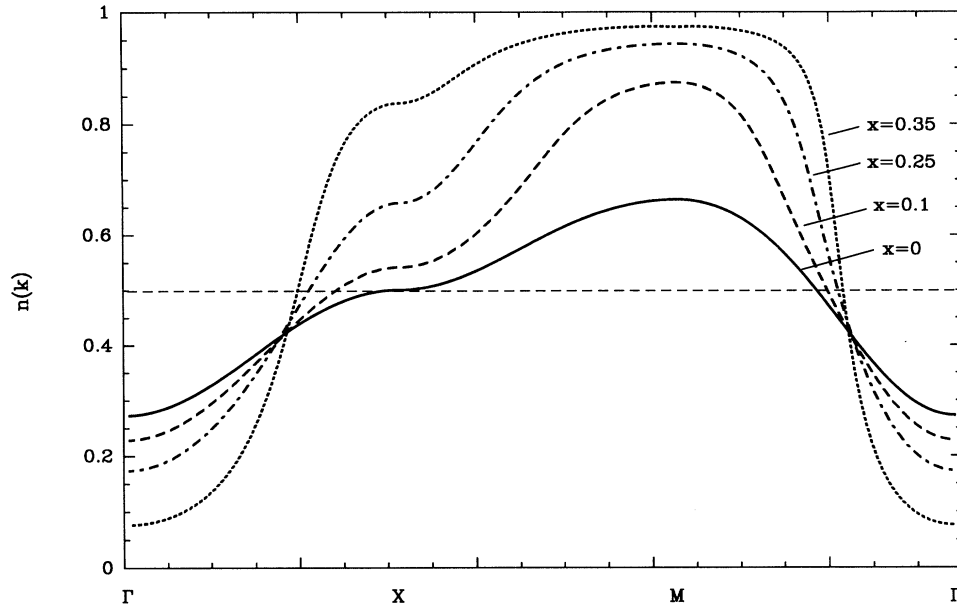


FIG. 6. Results for the momentum distribution $n(k)$ for various hole concentrations. Note that the most significant changes of $n(k)$ upon doping do not occur at the Fermi surface where $n(k) = \frac{1}{2}$ but at the M and X points.

good quantum number in the CPA, the energy dispersion ε_k can be obtained approximately from the maximum of the momentum-dependent density of states, $\varrho(k, \omega)$. Despite their different physical origin the dispersion of

these bands is very similar to that of the lower band in a Pauli-paramagnetic Hartree-Fock calculation. This surprising fact is due to the bonding character of all these bands. However, in a Hartree-Fock calculation for $x = 0$

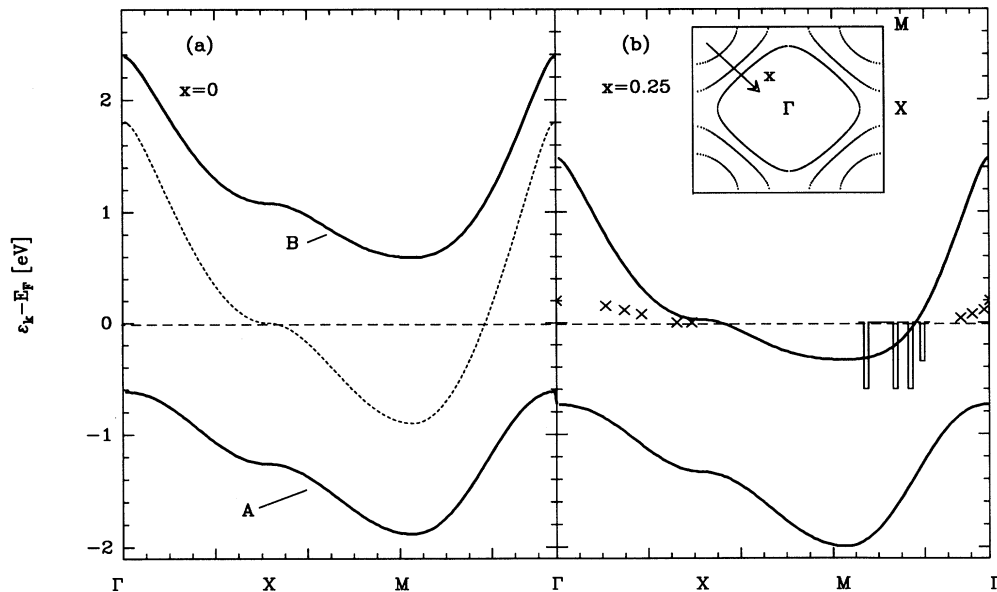


FIG. 7. Calculated dispersion (hole picture) of the lower Hubbard band (A) and the lower ligand hole band (B) in the paramagnetic phase for $x = 0$ (a) and $x = 0.25$ (b). The dashed line refers to the bonding band in the Pauli-paramagnetic state obtained using the Hartree-Fock approximation. Note that in the case of a Pauli-paramagnetic phase the Fermi level is in the middle of the band for half filling, whereas the local moment phase is insulating. The crosses denote electron states from ARPES's (Ref. 23) and the large bars (representing experimental resolution) hole states from ARPES's (Refs. 23 and 24). The inset shows the doping dependence of the effective Fermi surface obtained from $\varepsilon_k = E_F$. The arrow indicates increasing hole doping from $x = 0.1$ to $x = 0.25$ and $x = 0.35$.

the Fermi level is in the middle of the band, whereas the local moment phase is insulating. The k dependence of our energy dispersion is basically in agreement with photoemission data and exact cluster calculations. As can be seen from Fig. 7(b) our bandwidths are too large, and for $x = 0.25$ the position of E_F with respect to the X point is not correct. This is probably related to the fact that our mean-field theory does not yield an incoherent contribution to the spectral density. In exact cluster calculations a broad incoherent part of the spectrum is complemented by a very narrow coherent feature which disperses through the Fermi energy and which is rapidly filled upon doping.

It follows from the above results that the momentum states at the Fermi surface ($k = k_F$) differ from those with $\varepsilon_k = E_F$. The latter ones may define an effective Fermi surface which contains the momentum states near the Fermi energy. These states determine the behavior of the low-lying excitations and are mainly responsible for transport properties such as the Hall coefficient. The doping dependence of the *effective* Fermi surface is illustrated in the inset of Fig. 7. For small hole concentrations hole pockets near $k = (\pm\pi, \pm\pi)$ occur, which grow upon doping. For $x \approx 0.3$ (just before the charge-transfer gap vanishes) the character of the effective Fermi surface changes and we obtain a closed Fermi surface filled with electrons. Again, corresponding results are obtained for electron doping. Thus, for larger doping the effective Fermi surface and the Fermi surface defined from $n(k)$ coincide. For $x < 0.3$ the two Fermi surfaces are different. By contrast, in exact cluster calculations¹⁰ for $x \approx 0.1$ the Fermi surface determined from ε_k is already closed.

We conclude that our Fermi surface determined from $n(k)$ is in agreement with cluster calculations, since $n(k)$ is determined from all contributions to the spectrum. By contrast, for determining the Fermi surface from the energy dispersion it is important to distinguish between the coherent and the incoherent parts of the spectrum. Nevertheless, we expect that for very small doping the *effective* Fermi surface consists of hole or electron pockets even if a significant part of the spectrum is incoherent. For large doping we have already argued that our theory should yield satisfactory results. Thus, we consider our results for intermediate doping as an interpolation between those obtained for large and very small carrier concentrations.

In Fig. 8 we show the doping dependence of the Hall coefficient calculated within the Kubo formalism for disordered alloys⁵¹ which is independent of the actual definition of the Fermi surface. Concerning the validity of our theory it is significant that our results for R_H are in good quantitative agreement with experiment.¹⁸⁻²⁰ We obtain in particular the sign change of the Hall coefficient upon electron or hole doping. The sign change and the divergence of the Hall coefficient appear to be inconsistent with the doping dependence of the Fermi surface shown in Fig. 5. However, since the transport properties are determined by the states at the Fermi energy, the curvature of the *effective* Fermi surface is responsible for the doping dependence of the Hall coefficient. This can be seen from the agreement of our results for R_H obtained from the Kubo formalism with those determined from the energy dispersion and the Boltzmann equation following Ref. 52; see Fig. 8. For example, the hole pockets of the effective Fermi surface near $k = (\pm\pi, \pm\pi)$ lead to a

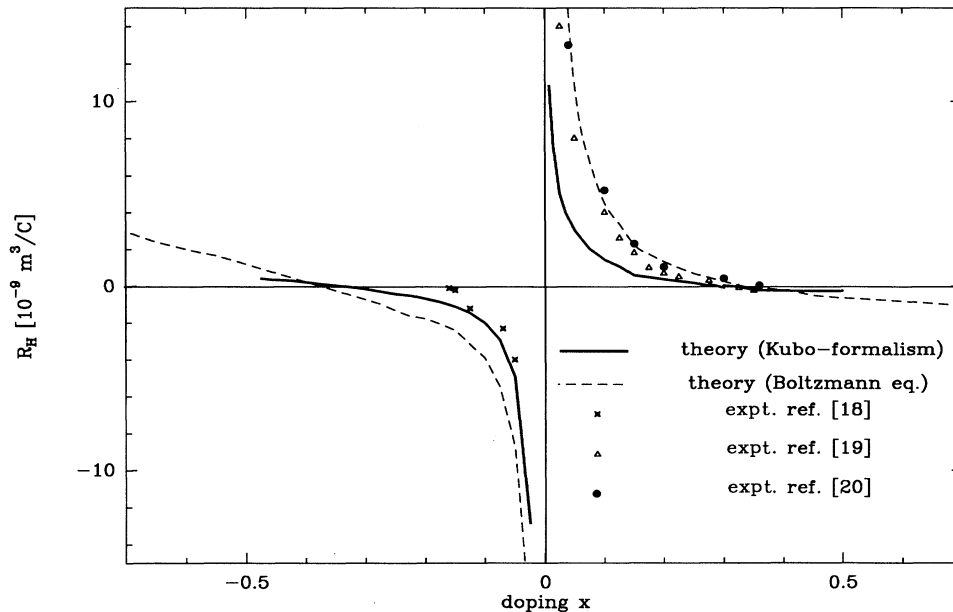


FIG. 8. Theoretical results for the Hall coefficient R_H of electron-doped ($x < 0$) and hole-doped ($x > 0$) CuO_2 planes are compared with experimental data. The solid lines show our results obtained from the Kubo formalism for disordered alloys. The dashed lines refer to results calculated from the relaxation time approximation of the Boltzmann equation and the dispersion of the bands shown in Fig. 7.

negative effective mass of the electrons and a divergence of the Hall coefficient.⁵³ For larger doping the effective Fermi surface is closed and the electrons have a positive effective mass, causing the sign change of R_H . Despite the above-mentioned uncertainties concerning our results for the effective Fermi surface, we believe that we correctly describe the divergent behavior of R_H for very small doping and the occurrence of a sign change for larger doping. The rapid formation of a large effective Fermi surface upon doping is due to the fact that the momentum states with a maximum in $\rho(k, \omega)$ close to the top of the lower Hubbard band (relevant in the case of electron doping) or the bottom of the lower ligand hole band (relevant for hole doping) have only a relatively small weight within the respective subband. Consequently, the intriguing doping dependence of R_H may result from an unusual behavior of the Fermi surface in a slightly doped charge-transfer system where the bands are split due to strong correlations.

IV. CONCLUSIONS

We have presented a mean-field theory which describes the transition from local magnetic moment to itinerant behavior in the CuO_2 planes. The theory is able to treat the whole doping range and indicates clearly the significance of local magnetic moments for the electronic structure. The essential approximations are the slave-boson saddle-point approximation which neglects quantum fluctuations and the CPA for treating the site dependence of the magnetic molecular field. We have compared our results in detail with experimental data and with alternative calculations. From this we conclude that we can correctly describe the metal-insulator transition, the energy dispersion of the bands, the Cu-O singlet formation, and the doping dependence of the Fermi surface [defined by $n(k) = \frac{1}{2}$]. Our results for the doping dependence of the density of states and of the Hall coefficient are also in satisfactory agreement with experiment. In order to distinguish between coherent and incoherent contributions to the spectral density it will be important to include quantum fluctuations following the treatment of our previous work.

Summarizing, we have developed a mean-field approach to the paramagnetic phase of a strongly correlated system which differs from the conventional slave-boson saddle-point approximations, where the magnetic molecular field is neglected. The approach has important consequences for systems close to half filling, since it leads to a metal-insulator transition resulting from band splitting. This is different from the Brinkmann-Rice localization obtained in the slave-boson mean-field theory for the Pauli-paramagnetic phase. Note that we do not *a priori* exclude this localization, but it does not occur for energetical reasons.

It is important that our model can be straightforwardly extended to describe the asymmetric behavior of the antiferromagnetic phase upon electron or hole doping³⁰ and also the unusual doping and temperature dependence of the static spin susceptibility³¹ if we take into account possible short-range magnetic order in the local moment phase. For electron-doped systems we then find a breakdown of the three-dimensional antiferromagnetism and a transition to the paramagnetic phase with local magnetic moments at $x_c = 0.09$ (experiment,¹ $x_c \simeq 0.14$) due to magnetic dilution. In hole-doped systems the carriers go to the oxygen sites and the three-dimensional antiferromagnetism is destroyed by singlet-induced frustration at $x_c = 0.025$ (experiment,¹ $x_c \simeq 0.02$). For $x > 0.03$ pronounced two-dimensional short-range order occurs. Correspondingly, the spin susceptibility for small hole doping and at low temperatures is suppressed due to antiferromagnetic correlations. For intermediate doping, when the magnetic correlations between the local moment are small, we obtain a Curie-Weiss-like behavior of the susceptibility. For $x > 0.4$ the magnetic moments disappear and we find temperature-independent Pauli susceptibility. This behavior is in good agreement with experimental results.

ACKNOWLEDGMENTS

This work was supported in part by the Bundesministerium für Forschung und Technologie through the project "HTSL-elektronische Vorgänge" and by the Deutsche Forschungsgemeinschaft.

-
- ¹ G. M. Luke *et al.*, Phys. Rev. B **42**, 7981 (1990).
² C. H. Pennington *et al.*, Phys. Rev. B **39**, 277 (1989); Y. Kitaoka *et al.*, Prog. Theor. Phys. Suppl. **101**, 371 (1990).
³ R. J. Birgeneau *et al.*, Phys. Rev. B **38**, 6614 (1988); J. Rossat-Mignod *et al.*, Physica C **169**, 58 (1991).
⁴ S. L. Cooper *et al.*, Phys. Rev. B **42**, 10785 (1990).
⁵ C. T. Chen *et al.*, Phys. Rev. Lett. **66**, 104 (1991).
⁶ H. Romberg *et al.*, Phys. Rev. B **42**, 8768 (1990).
⁷ J. Allen *et al.*, Phys. Rev. Lett. **64**, 595 (1990).
⁸ M. A. van Veenendal, R. Schlatmann, G. A. Sawatzky, and W. A. Groen, Phys. Rev. B **47**, 446 (1993).
⁹ J. Wagner, W. Hanke, and D. J. Scalapino, Phys. Rev. B **43**, 10517 (1991).
¹⁰ W. Stephan and P. Horsch, Phys. Rev. Lett. **66**, 2258 (1991).
¹¹ H. Eskes, M. B. J. Meinders, and G. A. Sawatzky, Phys. Rev. Lett. **67**, 1035 (1991).
¹² T. Tohyama and S. Maekawa, Physica C **191**, 193 (1992).
¹³ E. Dagotto, F. Ortolani, and D. Scalapino, Phys. Rev. B **46**, 3183 (1992).
¹⁴ M. Imada and Y. Hatsugai, J. Phys. Soc. Jpn. **58**, 3752 (1989).
¹⁵ A. Moreo and D. J. Scalapino, Phys. Rev. B **43**, 8211 (1991).
¹⁶ G. Dopf, A. Muramatsu, and W. Hanke, Phys. Rev. Lett. **68**, 353 (1992).
¹⁷ M. S. Hybertsen and L. F. Mattheis, Phys. Rev. Lett. **60**, 1661 (1988).

- ¹⁸ H. Takagi, S. Uchida, and Y. Tokura, *Phys. Rev. Lett.* **62**, 1197 (1989).
- ¹⁹ H. Takagi *et al.*, *Phys. Rev. B* **40**, 2254 (1989).
- ²⁰ M. Suzuki, *Phys. Rev. B* **39**, 2312 (1989).
- ²¹ T. Takahashi *et al.*, *Phys. Rev. B* **39**, 6636 (1989).
- ²² C. G. Olson *et al.*, *Phys. Rev. B* **42**, 381 (1990).
- ²³ G. Mante *et al.*, *Z. Phys. B* **80**, 181 (1990).
- ²⁴ R. Claessen *et al.*, *Phys. Rev. B* **39**, 7316 (1989).
- ²⁵ P. Lacour-Gayet and M. Cyrot, *J. Phys. C* **7**, 400 (1974).
- ²⁶ J. Hubbard, *Phys. Rev. B* **19**, 2626 (1979); H. Hasegawa, *J. Phys. Soc. Jpn.* **46**, 1504 (1979); see also *Electron Correlations and Magnetism in Narrow-Band-Systems*, edited by T. Moriya (Springer, Berlin, 1981).
- ²⁷ J. Schmalian, G. Baumgärtel, and K.-H. Bennemann, *Phys. Rev. Lett.* **68**, 1406 (1992).
- ²⁸ A. P. Kampf, *Phys. Rev. B* **44**, 2637 (1991).
- ²⁹ F. Yndurain and G. Martinez, *Phys. Rev. B* **43**, 3691 (1991); W. Zhang, M. Avignon, and K. H. Bennemann, *ibid.* **B 45**, 12478 (1992).
- ³⁰ J. Schmalian, G. Baumgärtel, and K.-H. Bennemann *Solid State Commun.* **86**, 119 (1993).
- ³¹ G. Baumgärtel, J. Schmalian, and K.-H. Bennemann (unpublished).
- ³² F. C. Zhang and T. M. Rice, *Phys. Rev. B* **37**, 3759 (1988).
- ³³ Y. Ohta, T. Tohyama, and S. Maekawa, *Phys. Rev. Lett.* **66**, 1228 (1991).
- ³⁴ T. Li, P. Wölfle, and P. J. Hirschfeld, *Phys. Rev. B* **40**, 6817 (1989).
- ³⁵ G. Kotliar and A. E. Ruckenstein, *Phys. Rev. Lett.* **57**, 1362 (1986).
- ³⁶ H. Shiba, *Prog. Theor. Phys.* **46**, 77 (1971).
- ³⁷ H. Hasegawa, *J. Phys. Condens. Matter* **1**, 9325 (1989).
- ³⁸ L. Lilly, A. Muramatsu, and W. Hanke, *Phys. Rev. Lett.* **65**, 1379 (1990).
- ³⁹ E. N. Economou, *Green's Functions in Quantum Physics* (Springer, Berlin, 1979), p. 88.
- ⁴⁰ B. Velicky, *Phys. Rev.* **184**, 614 (1969).
- ⁴¹ Of course, this is expected on general physical grounds. However, since some cluster calculations (Refs. 9 and 12) seem to find for $\Delta/U < 1$ that the singlet band is dominated by Cu states, we stress here that we obtain an oxygen-dominated singlet band.
- ⁴² W. F. Brinkmann and T. M. Rice, *Phys. Rev. B* **2**, 4302 (1970); C. Balseiro, M. Avignon, A. Rojo, and B. Alascio, *Phys. Rev. Lett.* **62**, 2624 (1989); R. Hayn and R. Schumann, *Physica C* **174**, 199 (1991).
- ⁴³ A. Oguri and T. Asahata, *Phys. Rev. B* **46**, 14073 (1992).
- ⁴⁴ Y. Ohta, K. Tsutsui, W. Koshibae, T. Shimozato, and S. Maekawa, *Phys. Rev. B* **46**, 14022 (1992).
- ⁴⁵ G. Mante, Th. Schmalz, R. Manzke, M. Skibowski, M. Alexander, and J. Fink (unpublished).
- ⁴⁶ W. Alexander *et al.*, *Phys. Rev. B* **43**, 333 (1991).
- ⁴⁷ H. E. Castillo and C.A. Balseiro, *Phys. Rev. Lett.* **68**, 121 (1992).
- ⁴⁸ M. E. Simon and A. A. Aligia, *Solid State Commun* **85**, 213 (1993).
- ⁴⁹ R. R. P. Singh and R. L. Glenister, *Phys. Rev. B* **46**, 14313 (1992).
- ⁵⁰ This conclusion does not apply to exact cluster-diagonalization studies where a significant part of the spectrum contributing to $n(k)$ is incoherent.
- ⁵¹ K. Niizeki and K. Hoshino, *J. Phys. C* **9**, 3481 (1976).
- ⁵² P. B. Allen, W. E. Pickett, and H. Krakauer, *Phys. Rev.* **37**, 7482 (1988).
- ⁵³ H. Fukuyama and Y. Hasegawa, *Physica B&C* **148**, 204 (1987).